View metadata, citation and similar papers at core.ac.uk

brought to you by CORE

provided by AIR Universita degli studi di Milano

Journal of Cellular Physiology

Zebrafish Tmem230a cooperates with the Delta/Notch signaling pathway to modulate endothelial cell number in angiogenic vessels

Journal:	*Journal of Cellular Physiology*
Manuscript ID	Draft
Wiley - Manuscript type:	Original Research Article
Date Submitted by the Author:	n/a
Complete List of Authors:	Carra, Silvia; University of Milan, Biosciences Sangiorgio, Lorenzo; University of Milan, Biosciences Pelucchi, Paride; Istituto di Tecnologie Biomediche Consiglio Nazionale delle Ricerche, Cancer Stem Cell Research Cermenati, Solei; University of Milan, Biosciences Mezzelani, Alessandra; Istituto di Tecnologie Biomediche Consiglio Nazionale delle Ricerche, Cancer Stem Cell Research martino, valentina; Istituto di Tecnologie Biomediche Consiglio Nazionale delle Ricerche, Cancer Stem Cell Research Palizban, Mira; Istituto di Tecnologie Biomediche Consiglio Nazionale delle Ricerche, Cancer Stem Cell Research Albertini, Alberto; Istituto di Tecnologie Biomediche Consiglio Nazionale delle Ricerche, Cancer Stem Cell Research goette, martin; University of Münster Kehler, James; National Institutes of Health Deflorian, Gianluca; IFOM-IEO Campus Beltrame, Monica; University of Milan, Biosciences Giordano, Antonio; Temple University, Sbarro Institute for Cancer Research and Molecular Medicine, Center for Biotechnology, College of Science and Technology; University of Siena, Department of Medicine, Surgery and Neuroscience University of Siena, Siena, Italy Cotelli, Franco; University of Milano, Biology reinbold, rolland; Istituto di Tecnologie Biomediche Consiglio Nazionale delle Ricerche, Cancer Stem Cell Research Bellipanni, Gianfranco; College of Science and Technology Temple University, Sbarro Institute for Cancer Research and Molecular Medicine ; College of Science and Technology Temple University, Department of Biology zucchi, ileana; Istituto di Tecnologie Biomediche Consiglio Nazionale delle Ricerche, Cancer Stem Cell Research
Key Words:	Angiogenesis, Delta/Notch signaling, Vegfc/Flt4 signaling, Regenerative Medicine, blood vessel formation growth

SCHOLARONE™
Manuscripts

For Peer Review

Zebrafish Tmem230a cooperates with the Delta/Notch signaling pathway to modulate endothelial cell number in angiogenic vessels

Silvia Carra[1,2#], Lorenzo Sangiorgio[1,2#], Paride Pelucchi[2#], Solei Cermenati[1], Alessandra Mezzelani[2], Valentina Martino[2], Mira Palizban[2], Alberto Albertini[2], Martin Götte[3], James Kehler[2,4], Gianluca Deflorian[5], Monica Beltrame[1], Antonio Giordano[6], Franco Cotelli[1*], Rolland Reinbold[2], Gianfranco Bellipanni[6] and Ileana Zucchi[2*]

1. Dipartimento di Bioscienze, Università degli Studi di Milano, Via Celoria 26, Milano 20133, Italy
2. Istituto di Tecnologie Biomediche, Consiglio Nazionale delle Ricerche, via F.lli Cervi 93, Segrate-Milano 20090, Italy
3. Department of Gynecology and Obstetrics, Muenster University Hospital, Muenster D48149, Germany
4. National Institute of Diabetes and Digestive and Kidney Diseases, National Institutes of Health, Bethesda 20814, USA
5. IFOM-IEO Campus, Via Adamello 16, Milano 20139, Italy
6. Center for Biotechnology, Sbarro Institute for Research and Molecular Medicine and Department of Biology, Temple University, Philadelphia 19122, USA
#First authors with equal contribution

* Corresponding authors with equal contribution

Contact Information:
silvia.carra@unimi.it
lorenzo.sangiorgio@gmail.com
paride.pelucchi@itb.cnr.it
solei.cermenati@unimi.it
alessandra.mezzelani@itb.cnr.it
valentina.martino@itb.cnr.it
mirapalizban@hotmail.com
alberto.albertini@itb.cnr.it
martingotte@uni-muenster.de
james.kehler@icloud.com
gianluca.deflorian@ifom.eu
monica.beltrame@unimi.it
antonio.giordano@temple.edu
bellipa4@temple.edu
rolland.reinbold@itb.cnr.it
franco.cotelli@unimi.it
ileana.zucchi@itb.cnr.it

For Peer Review

Abstract

During embryonic development, new arteries and veins form from preexisting vessels in response to specific angiogenic signals. Angiogenic signaling is complex since not all endothelial cells exposed to angiogenic signals respond equally. Some cells will be selected to become tip cells and acquire migration and proliferation capacity necessary for vessel growth while others, the stalk cells become trailer cells that stay connected with pre-existing vessels and act as a linkage to new forming vessels. Additionally, stalk and tip cells have the capacity to interchange their roles. Stalk and tip cellular responses are mediated in part by the interactions of components of the Delta/Notch and Vegf signaling pathways. We have identified in zebrafish, that the transmembrane protein Tmem230a is a novel regulator of angiogenesis by its capacity to regulate the number of the endothelial cells in intersegmental vessels by co-operating with the Delta/Notch signaling pathway. Modulation of Tmem230a expression by itself is sufficient to rescue improper number of endothelial cells induced by aberrant expression or inhibition of the activity of genes associated with the Dll4/Notch pathway in zebrafish. Therefore, Tmem230a may have a modulatory role in vessel-network formation and growth. Our study supports that the activity of Tmem230a is through restricting Vegfc/Flt4 signaling. As the Tmem230 sequence is conserved in human, Tmem230 may represent a promising novel target for drug discovery and for disease therapy and regenerative medicine in promoting or restricting angiogenesis.

For Peer Review

Introduction

In embryonic development two distinct processes take place to form the vascular tree. New vessels form *de novo* for the assembly of mesoderm-derived endothelial precursors (angioblasts) that differentiate into a primitive vascular labyrinth (vasculogenesis). Subsequently, vessel sprouting allows the formation of smaller size vessels (angiogenesis) necessary for growth of a vascular tree necessary creating a network that remodels into arteries and veins(Adams and Alitalo, 2007).

Growth of a vascular tree requires the coordinated control of different functions including proliferation, directional migration and patterning of endothelial cells (ECs). Angiogensis is orchestrated by the regulatory interactions between the vascular endothelial growth factor (Vegf) and Notch signaling pathways that finely control the behavior and positional fate of ECs and determine which cells become tip or stalk behaving cells (Phng and Gerhardt, 2009) (Eilken and Adams, 2010).

The exposure of vessels to pro-angiogenic signals such as Vegf induces the tip cell phenotype only in a fraction of the ECs (Phng and Gerhardt, 2009) (Eilken and Adams, 2010). Tip cell behaviour is strongly controlled by the Notch pathway. Activation of Notch signaling occurs predominantly in stalk cells and takes place by the interaction of Notch with its ligand delta-like 4, Dll4, leading to the down-regulation of both the Vegfa and Vegfc receptors (Vegfr-2 and Vegfr-3/Flt4, respectively) in these cells (Hellstrom, 2007; Lobov, 2007; Tammela et al., 2008). Therefore, cells with higher levels of Dll4, low Notch activity and strong Vegf receptor transcription are thought to convert into tip cells. (Phng and Gerhardt, 2009).

For Peer Review

We identified two *tmem230* paralogous genes in zebrafish, *tmem230a* and *tmem230b,* and investigated their expression patterns and determined that *tmem230a* is expressed in the vascular districts in early zebrafish development. Our data reveal that Tmem230a regulates the number of endothelial cells in vessels formed through angiogenic processes by cooperating with the Delta/Notch signalling pathway. In this capacity Tmem230a may have a modulatory role in vessel-network formation and growth.

As only a fraction of the ECs acquires angiogenic behavior required for blood vessel branching, the identification of novel regulators of angiogenesis contributes to a better understanding of both the complex multifaceted regulation of angiogenesis in normal and pathological conditions. Signficantly, as the *tmem230a* sequence is conserved in mammals, TMEM230 may represent a new target for human therapy, in promoting or restricting angiogenesis in acute injury and chronic disease, and since blood vessel formation is also required for promoting tumor growth, invasion and metastasis, TMEM230 may also represent a novel target for human cancer therapy.

For Peer Review

Materials and Methods

Zebrafish lines and maintenance.

Zebrafish (*Danio rerio*) embryos obtained from natural spawning were raised and maintained according to established techniques(Westerfield, 1993). All experiments with live animals were performed at the University of Milan. All experimental protocols and methods were carried out in accordance with relevant guidelines and regulations of Good Animal Practice approved by the institutional and licensing committee IACUC (Institutional Animal Care and Use Committee) and University of Milan by the Italian

Decree of March 4th 2014, n.26. Embryos were staged according to morphological criteria(Kimmel et al., 1995). Beginning from 24 hpf, embryos were cultured in fish water containing 0.003% PTU (1-phenyl-2-thiourea; Sigma Aldrich, Saint Louis, Mo, USA) to prevent pigmentation and 0.01% methylene blue to prevent fungal growth.

The following lines were used: AB (obtained from the Wilson lab, University College London, London, United Kingdom), tg(*fli1*:nEGFP)^{y7} (Roman et al., 2002), tg(*fli1*:EGFP)^{y1} (Lawson, 2002) (from the N.D. Lawson lab, University of Massachusetts Medical School, Boston, USA) and the reporter line Tg(T2KTp1bglob:hmgb1-mCherry)^{jh11} (from the Argenton Lab, University of Padua, Padua, Italy)(Schiavone et al., 2014) outcrossed with tg(*fli1*:EGFP)^{y1}.

***Tmem230* sequence analysis.**

Sequence analysis was performed using Genomic Database (www.ensembl.org) NCBI (http://www.ncbi.nlm.nih.gov/BLAST/) ClustalW (http://www.ebi.ac.uk/Tools/clustalw/) Genomicus (http://www.genomicus.biologie.ens.fr/genomicus-83.01/cgi-bin/search.pl). Prediction of transmembrane regions, topology and orientation analysis was performed using TMPRED (http://www.ch.embnet.org/software/TMPRED_form.html)(Hofmann, 1993) and HMMTOP (http://www.enzim.hu/hmmtop/index.php)(Tusnady and Simon, 2001).

Expression pattern analysis.

RT-PCR (Reverse Transcription-Polymerase Chain Reaction) was performed on total RNA prepared from zebrafish oocytes and embryos at different developmental stages using the Totally RNA Isolation Kit (Ambion, ThermoFisher, Waltham MA, USA) or the

For Peer Review

RNAgents Total RNA Isolation System (Promega, Madison, WI, USA), treated with DNase I RNase free (Roche, Basel, Switzerland) to avoid possible contamination from genomic DNA and then reverse transcribed using the ImProm-II Reverse Transcription System (Promega) and random primers. The cDNAs were then PCR amplified using GOTaq polymerase (Promega).

The following PCR primers were used: *tmem230a for*: 5'GCAGAGGATCGAGCAGTGTT 3', *tmem230a rev*: 5'GAAGGCAACACATGCAACAG 3', *tmem230b* left: 5' AGAAGATGCCTGCTCGAAGC 3', *tmem230b* right: 5' GCTGAGATCTCTGTCAGTCG 3'. Specific β□*actin* primers were used as internal control to check cDNA quality and possible genomic contamination(Argenton et al., 2004).

***In situ* hybridization and imaging.**

Whole-mount *in situ* hybridization (WISH) was performed as described(Thisse et al., 1993; Wu et al., 2011). For *tmem230a* and *tmem230b* probe preparations, templates spanning the last portion of coding sequence and the 3' UTR region for *tmem230a* or the entire coding sequence for *tmem230b* were generated by RT-PCR on total RNA extracted from 26 hpf embryos using the following primers: *tmem230a new1F*: 5' GCTTCCAAAGGTTACCGTGG 3' *tmem230a* new2R: 5' AAAGGCTTGGACACATCTGC 3' *tmem230b* left: 5' AGAAGATGCCTGCTCGAAGC 3' *tmem230b* right: 5' GCTGAGATCTCTGTCAGTCG 3'. PCR products were cloned into the *pGEM*®-T Easy vector (Promega).

For Peer Review

The cDNA-containing plasmids were linearized and transcribed with T7 and Sp6 RNA polymerase (Roche) for antisense and sense riboprobe synthesis.

Plasmid probes for *flk1(Fouquet et al., 1997)*, *flt4(Thompson et al., 1998)*, and *dll4(Siekmann and Lawson, 2007)* were kindly provided by N.D Lawson, and *efnb2a* and *ephB4(Lawson et al., 2001)* were kindly provided by R. Patient (Weatherall Institute of Molecular Medicine, University of Oxford, John Radcliffe Hospital, Oxford, U.K.). Images of stained embryos were taken with a Leica MZFLIII epifluorescence stereomicroscope equipped with a DFC 480-R2 digital camera using the LAS imaging software (Leica, Germany).

For histological sections, stained embryos were re-fixed in 4% PFA, dehydrated, wax embedded, sectioned (8 µm) by a microtome (Leitz 1516) and stained with eosin. Images were taken with a Leica DM6000 B microscope equipped with a Leica 480 digital camera using the LAS software (Leica, Germany).

Morpholino and mRNA injections and detection of splice variants of the *tmem230a* transcript by RT-PCR.

Two different antisense morpholinos (MOs) for *tmem230a* were synthesized by Gene Tools (Philomath, OR, USA): *tmem230a*-MO1 5' GTGTTGTTTCGGGTTGCCATCATA 3' and *tmem230a*-MO2 5' CAGCTTAGATATTTTCTCACCTGTA 3'. *tmem230a*-MO1 was designed on the region surrounding the AUG translation start codon of the transcript. *tmem230a*-MO2 was designed on the exon2/intron2 boundary. The following morpholino was already described: *dll4*-MO(Hogan, 2009). As a control for unspecific effects, each experiment

For Peer Review

was performed in parallel with a standard control morpholino control (std-MO) that has no target in zebrafish. All morpholinos were diluted in Danieau's solution(Nasevicius and Ekker, 2000) and injected at the 1–2 cell stage embryo. Rhodamine dextran (Molecular Probes) was usually co-injected as a tracer. After injection, embryos were raised in fish water (previously described) at 28ºC and observed up to the stage of interest. For a better observation, the injected embryos were anaesthetized using 0.016% tricaine (Ethyl 3-aminobenzoate methanesulfonate salt, Sigma Aldrich) in fish water. To assess the ideal concentration of morpholino we injected several dilutions and verified at 24 hpf the overall effects of the morpholino on embryo phenotype. The injection of *tmem230a*-MO1 at a concentration above or equal to 0.4 pmol/embryo led to morphological defects, such as head defects and bent tail (not shown), and increased mortality in a dose dependent manner (Supplementary Fig. S4a), suggesting the activation of unspecific mechanisms at those concentrations. While, at a concentration of 0.3 pmol/embryo and below the survival rate was high and the embryos had a normal morphology and development (Supplementary Fig. S4a). We proceded in a similar way to determine the concentration of splicing morpholino *tmem230a*-MO2 to inject and we found we could inject an higher dose (1pmol/embryo) of this morpholino with not apparent effects in the gross morphology of the embryo (Supplementary Fig S4b).

Images were acquired using a Leica MZFLIII epifluorescence stereomicroscope equipped with a DFC 480-R2 digital camera and the LAS imaging software (Leica, Germany).

At 29 hpf, total RNA was extracted from embryos injected with *tmem230a*-MO2 or std-MO with RNAgents Total RNA Isolation System (Promega). Reverse transcription was carried out with the ImProm-II Reverse Transcription System (Promega) and random

For Peer Review

primers. PCR was performed to detect splice variants of *tmem230a*. The following primers were used: *tmem230a for*: 5'GCAGAGGATCGAGCAGTGTT 3' and *tmem230a rev*: 5'GAAGGCAACACATGCAACAG 3'. RT-PCR products were then sequenced.

For *tmem230a* mRNA, the complete coding sequence was cloned into the $pCS2^{+}$ plasmid which was then digested with *Not*I and *in vitro* transcribed using the mMESSAGE mMACHINE kit (Ambion). Rescue experiments were performed with the co-injection of 1pmol/embryo *tmem230a*-MO2 and 400 pg/embryo *tmem230a* mRNA diluted in the Danieau's solution into 1-cell stage embryos.

Analysis of ISV cell number.

We scored ISV cell number by counting cell nuclei expressing the GFP in tg(*fli1*:nEGFP)^{y7} embryos at 29 hpf. We considered for our analysis the first 10 intersegmental vessels anterior to the anus. We mounted injected embryos of each sample in 1% low-melting agarose (adding some drops of tricaine as anaesthetic) and observed in every embryo the same group of ISVs. Images were taken with a confocal Leica TCS SP2 AOBS microscope, equipped with an argon laser, with a PL FLUOTAR 20X x 0.50 NA objective. The mean of the cell number was calculated by counting GFP positive nuclei in 10 segments/embryo for the number of embryos indicated by n. Standard error of mean (SEM) is indicated as vertical bars with caps.

DAPT treatment.

A 40 mM stock solution of DAPT (*N*-[*N*-(3,5-difluorophenacetyl-1-alanyl)]-*S*-phenylglycine *t*-butyl ester, γ-secretase inhibitor IX; Calbiochem, La Jolla, CA, USA)

For Peer Review

was diluted to a concentration of 200 µM in E3 embryo medium as described(Westerfield, 1993). *tmem230a* mRNA and std-MO injected embryos were dechorionated by pronase (Sigma Aldrich) treatment(Westerfield, 1993) and treated with DAPT from 17 hpf to 29 hpf at 28°C. As DAPT is prepared with DMSO, *tmem230a* mRNA and std-MO injected embryos were treated with E3 embryo medium containing the same concentration of DMSO used for the DAPT treated embryos.

Live-imaging analysis of Notch reporter expression.

To assay the capacity of Tmem230a to regulate Notch signalling, we injected *tmem230a*-MO1 into 1-cell stage embryos generated from crossing the transgenic line *Tg(T2KTp1bglob:hmgb1-mCherry)* with Tg*(fli1a:*EGFP*)*^{y1}. The level of mCherry fluorescence expression in the vessels of the embryos was scored by confocal microscopic analysis. We mounted five embryos at 48 hpf from each sample in 1.2% low-melting agarose (adding some drops of tricaine as anaesthetic) and observed in every embryo the same group of 3 ISVs up to the yolk extension. Images were taken with a Leica TCS SP2 confocal microscope, using a water-immersion objective 40X.

Statistical analysis.

Statistical analysis was performed with one-way ANOVA analysis of variance technique and with Dunnett's post test using GraphPad PRISM versions 5.0 and 6.0 (GraphPad, San Diego, CA, USA). In the graphs, * and ** mark statistically significant data with a p value <0.05 and <0.01, respectively. Statistically highly significant data, with a p value <0.001, are marked by ***.

For Peer Review

Results

Tmem230 identification and bioinformatic analysis

We have identified Tmem230 differentially expressed at the onset of in vitro differentiation of pluripotent mouse embryonic stem cells (mESCs) (manuscript in preparation, PP and RR). To identify the role of Tmem230 in the earliest stages of vertebrate embryogenesis, Tmem230 expression was modulated in zebrafish, as a model for embryo tissue and organ development.

The zebrafish genome encodes two *tmem230* genes, *tmem230a* (zgc:101123) on chromosome 10 and its paralogue *tmem230b* (zgc:162251) on chromosome 8. The analysis of *tmem230* genes across vertebrates revealed that both genes are orthologs of mammalian *Tmem230* and both genes may have arisen from a duplication event (Fig. 1a). The *tmem230a* and *b* transcripts are 1663 and 1019 bp in length and encode proteins of 120 and 115 amino acids, respectively (Fig. 1b). The Tmem proteins are highly related to each other (83% identity, Supplementary Fig. S1a). In addition, Tmem230a protein shares 76% identity with their respective human and mouse orthologs, while Tmem230b shares 74% identity with the human and 75% with the mouse ortholog, respectively. Transmembrane topology prediction analysis of conserved domains revealed that Tmem230a and b proteins contain 2 transmembrane domains (Supplementary Fig. S1b).

For Peer Review

tmem230a is expressed in blood vessels during embryonic and early larval zebrafish development.

Temporal expression of both zebrafish *tmem230* genes (*a* and *b*) was analyzed in embryonic and early larval development and in adult organs and tissues by RT-PCR analysis (Fig. 2a and Supplementary Fig. S2a). Both transcripts were detected at all analyzed stages from cleavage up to 5 dpf, as well as in oocytes, suggesting that both transcripts are both maternally and zygotically expressed. Furthermore, *tmem230a* and *tmem230b* expression was detected in all adult organs and tissues tested (brain, eyes, gills, gut, heart, liver and muscle). Whole-mount *in situ* hybridization (WISH) analysis revealed that from the mid somitogenesis stage (15 somites) to 2 dpf, *tmem230a* has higher expression in the developing vascular system than *tmem230b* (Fig. 2b-j and Supplementary Fig. S2b-f). At the 15 somite stage, *tmem230a* was expressed in the telencephalon, mesencephalon and hindbrain, and was starting to be expressed in the Intermediate Cell Mass (ICM) and in the forming axial vasculature (Fig. 2b). At 26 hpf, *tmem230a* was expressed in the pharyngeal arch mesenchyme, in the Dorsal Aorta (DA) and Caudal Vein (CV) (Fig. 2c,c',d,h,i). At 2 dpf, a strong hybridization signal was detected at the level of the mandibular arches and in the fin buds, and moreover *tmem230a* was expressed at low levels in the CV plexus region (Fig. 2e,f,g,j). In contrast, no hybridization signal was detected for *tmem230b* in the forming vasculature (Supplementary Fig. S2b-f). During somitogenesis (15 to 20 somite stages), WISH staining revealed a faint and ubiquitous *tmem230b* hybridization signal (Supplementary Fig. S2b,c). At the 15 somite stage, *tmem230b* expression appeared fairly widespread, while at the 20 somite stage was expressed in the tail and eyes. At 26 hpf, *tmem230b* was

For Peer Review

detectable in the optic tectum, mesencephalon, hindbrain and in the tail including the CV region and in the somites (Supplementary Fig. S2d, d',e). At 2 dpf, *tmem230b* was only slightly expressed in the mesencephalon (Supplementary Fig. S2f).

Since our data indicate a robust *tmem230a* expression in the developing vasculature not overlapping with the expression of *tmem230b*, we investigated the role of Tmem230a in vascular development.

Tmem230a modulates ISV endothelial cell number.

To determine the role of *tmem230a,* we first looked to the effects of *tmem230a* knock-down, to reduce Tmem230a protein in the developing vasculature. To not interfere with the early embryonic expression of *tmem230a,* a gene knockdown approach with morpholinos was used. Knockdown experiments were performed by independent injections of two different morpholinos: a low dose *tmem230a*-MO1 and *tmem230a*-MO2, designed to block mRNA translation or splicing, respectively (Fig. 3). The sequences of both *tmem230a*-morpholinos were analyzed to exclude cross targeting to *tmem230b* (Supplementary Fig. S3a). We injected *tmem230a*-MO1 at the selected dose of 0.3 pmol/embryo and *tmem230a*-MO2 at 1pmol/embryo in one cell stage tg(*fli1*:nEGFP)^{y7} embryos. These concentrations of morpholinos did not affect the gross phenotype of the zebrafish embryos and the main axial vessels appeared normal in all injected embryos at 29 hpf and 2 dpf (Fig. 3 and see Methods and Supplementary Figs. S4 and S5). The injections in transgenic embryos tg(*fli1*:nEGFP)^{y7} allowed for the quantification of intersegmental vessel (ISV) cell numbers by counting cell nuclei expressing the green fluorescent protein (GFP) (Fig. 3 a-g). We counted cells in the first 10 intersegmental vessels anterior to the anus and found a statistically significant increase

For Peer Review

of the mean number of cells in ISVs when tg(*fli1*:nEGFP)^{y7} embryos were injected with 0.3 pmol MO1 (n = 100) compared to control std-MO injected embryos (n = 69) (Fig. 3e,k)(Roman et al., 2002). To further confirm these results, when we injected the splice-blocking *tmem230a*-MO2 at 1 pmol/embryo in the same transgenic line embryos, we observed a comparable increase in ISV cell number though with a different penetrance (Supplementary Fig. S4b and Fig. 3e,i,l). The injection of *tmem230a*-MO2 which targets the exon2-intron2 boundary, generated a transcript unable to splice exon 2 from intron 2 (Supplementary Fig. S3b). Sequencing of the smaller PCR product confirmed a sequence skipping *tmem230a* exon 2 consistent with a previous report showing that targeting of a E2/I2 junction may result in exon 2 skipping (Morcos, 2007). This mRNA having no starting codon in frame with the *tmem230a* sequence yields a non-functional *tmem230a* mRNA.

In parallel to the loss-of-function experiments, mRNA over-expression experiments were performed. We injected *tmem230a* mRNA (400 pg/embryo) in one cell stage tg(*fli1*:nEGFP)^{y7} embryos. As for the knock-down experiments, we counted the number of ISV cells present in the first 10 intersegmental vessels anterior to the anus. Consistent with the phenotype observed with the loss-of-function of Tmem230a, the gain-of-function experiment resulted into the opposite phenotype. We found a statistically significant ($p<0.0001$) decrease of the mean number of cells in ISVs in the tmem230a-over-expressing embryos (29.17 mean ISV cells present in the first 10 intersegmental vessels anterior to the anus for the tmem230a over-expressing embryos, n = 60, versus 35.06 mean cell number for the control, n = 32), (Fig. 3 j,k).

For Peer Review

Experiments using two independent morpholinos at concentrations that did not result in gross morphological defects, both gave the same *in vivo* phenotype affecting the ISV cell number. In addition, Tmem230a gain and loss of function experiments consistently produced opposite effects on the ISV cell number. Moreover, we fully rescued the effects on ISV cell number of injections of 1 pmol/embryo of *tmem230a*-MO2 by *tmem230a* mRNA over-expression (400 pg/embryo) (Fig. 3l).

Taken together these data suggest a *bona fide* role of *tmem230a* in regulating ISV cell number during angiogenesis. Considering that both morpholinos produced the same phenotypes, we performed all following experiments by injecting *tmem230a*-MO1 into embryos, which we indicate as *tmem230a* morphants.

Tmem230a knockdown affects angiogenic blood vessel growth rather than artero-venous endothelial cell fate.

The effect of Tmem230a in ISV cell number could be explained in two possible ways: either Tmem230a affects blood vessel growth or regulates artero-venous cell fate switch. To gain insight into the molecular events following *tmem230a*-MO1 injection, we analyzed the expression of different vascular markers: *ephrin-B2* (*efnb2a*) and its receptor e*phB4*, specifically expressed in arterial and venous endothelium, and *flk1* (vegf receptor 2, *vegfr2*), *flt4* (vegf receptor 3, *vegfr3*) and *dll4* (notch ligand delta-like 4) which are preferentially expressed in tip rather than in stalk cells(Adams and Alitalo, 2007; Blanco and Gerhardt, 2013; Fouquet et al., 1997; Gerety et al., 1999; Lawson et al., 2001; Phng and Gerhardt, 2009; Shutter et al., 2000; Siekmann and Lawson, 2007;

For Peer Review

Thompson et al., 1998; Wang, 1998). In std-MO and *tmem230a*-MO1 injected embryos, *efnb2a* and e*phb4* expression levels were comparable (for *efnb2a* n=74, n=75 respectively and for e*phb4* n=77, n=76, respectively; Fig. 4a-d). In contrast, increase of *flk1*, *flt4*, and *dll4* staining in ISVs and in the Dorsal Longitudinal Anastomotic Vessels (DLAVs) was observed in *tmem230a* morphants (for *flk1* 83% n=57; for *flt4* 79% n=52; and for *dll4* 53% n=44, respectively) compared with control embryos (for *flk1* n=16; for *flt4* n=19; and for *dll4* n=18; Fig. 4e-j).

No change in *efnb2a* and e*phB4,* but increase in *flk1*, *flt4*, and *dll4* marker levels in *tmem230a* morphants strongly suggests that more ISV cells were generated by *tmem230a*-MO1 injection. These results provided support that the role of *tmem230a* is restricted to angiogenic blood vessel growth and that *tmem230a* promotes angiogenic cell behavior rather than the determination of artero-venous cell fates. The increase of cell number can be due to various cellular processes including increase in cell proliferation and/or a result of cellular migration of ISV cells from the aorta.

Tmem230a and the Notch/Delta signaling pathway cooperate in modulating ISV endothelial cell number.

Previous studies have demonstrated that Notch restricts angiogenesis and that loss of the Notch ligand *dll4* led to supernumerary endothelial cells within the ISA(Leslie et al., 2007; Siekmann and Lawson, 2007). As *tmem230a* mRNA over-expression reduced ISV cell number, we wanted to determine whether *tmem230a* is involved in the Notch signaling pathway, and whether it acts synergistically with *dll4* in regulating the ISV cell number. Two independent approaches were used to answer these questions. First, we co-

For Peer Review

injected into embryos subcritical doses of *tmem230a*- (0.07 pmol/embryo) and *dll4*- (0.09 pmol/embryo) MOs (Fig. 5a-f). Results show that the subcritical doses of each morpholino do not cause alterations in ISV cell number when injected separately (Fig. 5e). However, when subcritical doses of both *dll4*- and *tmem230a*-MOs were co-injected into the same embryos a statistically significant increase in ISV cell number was observed, suggesting a synergistic effect of Dll4 and Tmem230a (Fig. 5c,e). Consistent with a role of Tmem230a in regulating ISV cell number, co-injection of *tmem230a* mRNA (400 pg/embryo) together with *dll4*-MO (0.4 pmol/embryo) rescued normal endothelial cell numbers in ISVs (Fig. 5d,f). As Dll4 is part of the Notch pathway and Notch restricts angiogenesis we hypothesized that a second and independent way to block Notch signaling would also produce the same results. Therefore, we investigated the effect of *tmem230a* in a context where the Notch signaling was blocked by using the γ-secretase inhibitor, DAPT(Geling et al., 2002). Consistent with the results obtained with the *dll4*-morphants, embryos treated with 200 μM DAPT showed an increase in the number of ISV cells compared to DMSO-control treated embryos (Fig. 5g). Embryos injected with *tmem230a* mRNA and treated with DAPT showed a number of ISV cells comparable to that of std-MO injected control embryos treated with DMSO, while DMSO-control embryos injected with *tmem230a* mRNA showed a decrease in ISV cell number as previously seen (Fig. 3j,k). These results confirm that embryos over-expressing *tmem230a* can rescue back the correct number of ISV cells in Notch signaling blocked embryos (Fig. 5g). Taken together, these data are consistent with the hypothesis that Tmem230a acts synergistically with Dll4 and has a role mediating Notch signaling pathway for ISV development.

For Peer Review

We further tested the effect of Tmem230a down regulation in Notch-responsive vessels *in vivo*. We injected *tmem230a*-MO1 into embryos obtained by the outcross of the transgenic line tg(*fli1*:EGFP)^{y1} with the transgenic line tg(*T2KTp1bglob:hmgb1-mCherry*)^{jh11} which expresses mCherry in tissues known to be Notch responsive. Expression of nuclear mCherry fluorescence protein occurs when the Notch intra-cellular domain (NICD) and its cofactor RBP-Jκ bind to the promoter of the Epstein Barr Virus terminal protein 1 (*TP1*) gene which contains two Rbp-Jκ binding sites(Parsons et al., 2009; Schiavone et al., 2014). For a better visualization of the activated *hmgb1-mCherry* we analyzed embryos at 48 hpf instead of the 29 hpf time point used for our previous experiments.

At 48 hpf, 76% (n = 98) of *tmem230a* morphants showed decrease of mCherry expression in ISVs and DA with respect to std-MO injected embryos (n = 125) (Fig. 6), strongly suggesting the involvement of Tmem230a in the positive modulation of Notch signaling in vascular districts responsive to Notch.

All results presented here support that Tmem230a has a modulatory role in the Dll4/Notch signaling pathway to limit angiogenic cell behavior.

Discussion

In zebrafish, embryonic trunk angiogenesis takes place in two distinct waves: formation of primary and secondary sprouts. From about 20 hpf, primary sprouts bilaterally form from the DA to give rise to intersegmental arterial (ISA) vessels, which are completed by 1.5 dpf. From about 32 hpf, secondary sprouts emerge from the posterior cardinal vein (PCV) to give rise to venous ISVs and lymphatic vascular precursors(Childs et al., 2002;

For Peer Review

Isogai et al., 2003; Yaniv et al., 2006). At 29-30 hpf, ISVs consist of three or four endothelial cells with different positional fates: a tip cell that is the dorsal-most T-shaped cell that contributes to the DLAV, an adjacent connector cell which is situated along the length of the medial somite boundary, and a base cell connected to the DA(Siekmann and Lawson, 2007). Growth of intersegmental veins requires the coordination of tip and stalk cell behaviors with different capacities for proliferation, directional migration, patterning and positional fates of ECs.

Here, we identified two *tmem230* paralogous genes in zebrafish. In this work, we investigated the expression pattern and the function of Tmem230a.

As our preliminary data (Fig. 2) indicated that *tmem230a* may have diverse functions since it was expressed throughout embryonic development including pre-gastrulation development, to focus only on the role of *tmem230a* in vascular development we decided to modulate *tmem230a* levels by morpholinos. In contrast to morpholinos, transgenic technologies and use of the CRISPR-Cas9 approach to induce mutations could produce early phenotypes, thus, mask later developmental events, like the vascular phenotype that we were interested to study (Blum et al., 2015). Injections of two independent *tmem230a*-MOs for the down regulation of Tmem230a led to the increase of endothelial cell number within the ISVs. Interestingly, over-expression of *tmem230a* mRNA resulted into the opposite phenotype, a marked decrease of endothelial cell number within the ISVs, supporting that the role of Tmem230a is to limit endothelial cell number and therefore modulate angiogenic vessel growth.

For Peer Review

The fact that two independent morpholinos resulted into the same phenotype and that the *tmem230a*-MO phenotype was rescued by *tmem230a* mRNA injection, demonstrated the specificity of the *tmem230a* morpholino obtained phenotypes.

The increase in number of ISV cells could be due to several events, such as increase in cell proliferation or a result of cellular migration of ISV endothelial cells from aorta which could be generally grouped in two main possibilities, changes in antero-venus cell fate or changes in precursors cell number. We showed here that *flk1*, *flt4*, and *dll4* staining in ISVs and in the Dorsal Longitudinal Anastomotic Vessels (DLAVs) increased and no difference in the arterial and venous marker expression were observed in *tmem230a* morphants compared to control embryos, suggesting that *tmem230a* does not regulate artero-venous cell fate specification but modulates the EC number in angiogenic blood vessels. It would be interesting to determine if these cells are generated by increased proliferation of local ISV cells or migration of ISV cells from aorta. We are planning to address this question in future work.

Different signals regulate tip and stalk cell behaviors by the interactions of genes associated to the Vegf and Notch signaling pathways(Eilken and Adams, 2010; Phng and Gerhardt, 2009). As the *tmem230a* morphants displayed the same ISV phenotype observed with *dll4* knockdown experiments previously described(Siekmann and Lawson, 2007), we investigated whether Tmem230a cooperates with, and/or modulates the Dll4/Notch signaling pathway in regulating angiogenesis. The co-injection of subcritical doses of *tmem230a*-MO1 and *dll4*-MO demonstrated that the down regulation of the two genes resulted in a synergistic increase of the ISV cell number, while the subcritical dose of *tmem230a*-MO1 or *dll4*-MO when injected individually, did not promote change in the

For Peer Review

number of ISV cells. Consistent with the subcritical co-injection results, a dose of *dll4*-MO higher than subcritical resulted in a supernumerary ISV cell number, whereas the *tmem230a* mRNA and *dll4*-MO co-injection rescued the phenotype generated by the *dll4*-MO higher dose. To further confirm the morpholino experiments, we decided to chemically block Notch signaling with DAPT treatment. The treated embryos displayed an excessive ISV cell number. In absence of Dll4 (*dll4*-MO) or with inhibition of Notch (NICD release with DAPT treatment), the injection of *tmem230* mRNA rescued the excessive ISV cell number, suggesting that *tmem230a* mRNA can independently compensate for the knockdown of *dll4* and inhibition of Notch. In agreement, decrease of mCherry expression under the control of Notch responsive elements was observed in vessels in *tmem230a* morphants supporting the involvement of *tmem230a*, like that for *dll4* in the positive modulation of Notch signaling.

These results strongly support that *tmem230a* has a role Dll4/Notch signaling. However, the precise epistatic relationships of *tmem230a* with respect the Dll4/Notch signaling in the modulation of EC numbers in ISVs still needs to be determined. In fact, our experiments suggest that *tmem230a* can compensate and/or cooperate with both the Dll4/Notch signaling pathways in limiting the number of endothelial cells in angiogenic processes in early development of zebrafish. Moreover, it still remains to be determined which components of the Dll4/Notch signaling pathways Tmem230a interacts with. For instance, does Tmem230a work with Notch as a co-receptor for Delta or cooperate with Notch within the cytoplasm for signal transduction. In order to answer these questions, co-localization of Tmem230a with Dll4/Notch signaling components need to be carried out.

For Peer Review

Our study is the first to identify TMEM230 as a novel regulator and modulator of angiogenesis associated blood vessel-network formation and growth. Recently, TMEM230 has been identified when mutated to have a role in Parkinson's disease. As to how TMEM230 mutation(s) contributes at the molecular level to the Parkinson's phenotype is still under investigation.(Baumann et al., 2017; Deng et al., 2016; Giri et al., 2017; He et al., 2016; Kim et al., 2017; Olszewska et al., 2016; Quadri et al., 2017; Wu et al., 2016; Yan et al., 2017). Our study is the first to associate and characterize TMEM230 to specific signaling pathways and provides first insight into how TMEM230 functions at the molecular level. Additionally, our study and the recent discovery of role of TMEM230 in Parkinson's disease suggest that novel genes with tantalizingly multiple functions in normal and disease vertebrate development are still to be discovered.

As the *tmem230a* gene sequence is conserved in vertebrates including human, and modulation of *tmem230a* expression alone was sufficient to rescue improper number of endothelial cells induced by aberrant expression levels of genes or by inhibition of gene activity in the Dll4/Notch pathway, this suggests that the TMEM230 protein is a novel and potentially clinically important alternative target for human regenerative therapy. For instance, extended modulation of TMEM230 expression by pharmacological agents may allow for inducing or mitigating new blood vessel formation for promoting following acute injury or restricting such as for macular degeneration in angiogenesis. As blood vessel formation is also essential for promoting tumor growth, circulation of cancer cells

For Peer Review

and metastasis, TMEM230 protein may also be a target for cancer therapy by repressing new blood vessel growth.

Declaration of conflict of Interest.

The authors declare that a patent application was submitted utilizing TMEM230 as a novel gene for regulation of human angiogenesis. Reinbold RA., Zucchi I. *Nuovi regolatori dell'angiogenesi,* patent application pending.

Acknowledgements

We like to thank Professor Federico Bussolino (University of Turin, Italy) for critical suggestions and Natascia Tiso (Argenton Lab, University of Padua, Padua, Italy) for providing the tg(T2KTp1bglob:hmgb1-mCherry)^{jh11} transgenic line. Funding for this research is provided to IZ: Cariplo Progetti-Internazionali 2008-2015 by Fondazione Cariplo; grants RBAP11BYNP and RBAP11Z4Z9 by MIUR-FIRB; and Progetto Bandiera Interomics. Silvia Carra, Lorenzo Sangiorgio and James Kehler were supported by fellowships from the Fondazione Cariplo to IZ.

Authors' Contributions

Comment [MOU1]:

SiCa, LS, and SoCe performed the zebrafish experiments and data analysis; PP, AM, VM and MP contributed tools for the experiments; GD performed experiments with the transgenic line tg(T2KTp1bglob:hmgb1-mCherry)^{jh11} crossed with the transgenic line

For Peer Review

tg(*fli1*:EGFP)^{y1}; JK, AA, MG provided critical advice and discussion; RR, FC, and IZ conceived the project. FC supervised all the Zebrafish experiments; SiCa, MB, AG, FC, GB, RR and IZ analyzed the data and wrote the paper.

For Peer Review

Literature Cited

Adams RH, Alitalo K. 2007. Molecular regulation of angiogenesis and lymphangiogenesis. Nat Rev Mol Cell Biol 8(6):464-478.

Argenton F, Giudici S, Deflorian G, Cimbro S, Cotelli F, Beltrame M. 2004. Ectopic expression and knockdown of a zebrafish sox21 reveal its role as a transcriptional repressor in early development. Mech Dev 121(2):131-142.

Baumann H, Wolff S, Munchau A, Hagenah JM, Lohmann K, Klein C. 2017. Evaluating the role of TMEM230 variants in Parkinson's disease. Parkinsonism Relat Disord 35:100-101.

Blanco R, Gerhardt H. 2013. VEGF and Notch in tip and stalk cell selection. Cold Spring Harb Perspect Med 3(1):a006569.

Blum M, De Robertis EM, Wallingford JB, Niehrs C. 2015. Morpholinos: Antisense and Sensibility. Dev Cell 35(2):145-149.

Childs S, Chen JN, Garrity DM, Fishman MC. 2002. Patterning of angiogenesis in the zebrafish embryo. Development 129(4):973-982.

Deng HX, Shi Y, Yang Y, Ahmeti KB, Miller N, Huang C, Cheng L, Zhai H, Deng S, Nuytemans K, Corbett NJ, Kim MJ, Deng H, Tang B, Yang Z, Xu Y, Chan P, Huang B, Gao XP, Song Z, Liu Z, Fecto F, Siddique N, Foroud T, Jankovic J, Ghetti B, Nicholson DA, Krainc D, Melen O, Vance JM, Pericak-Vance MA, Ma YC, Rajput AH, Siddique T. 2016. Identification of TMEM230 mutations in familial Parkinson's disease. Nat Genet 48(7):733-739.

Eilken HM, Adams RH. 2010. Dynamics of endothelial cell behavior in sprouting angiogenesis. Curr Opin Cell Biol 22(5):617-625.

Fouquet B, Weinstein BM, Serluca FC, Fishman MC. 1997. Vessel patterning in the embryo of the zebrafish: guidance by notochord. Dev Biol 183(1):37-48.

Geling A, Steiner H, Willem M, Bally-Cuif L, Haass C. 2002. A gamma-secretase inhibitor blocks Notch signaling in vivo and causes a severe neurogenic phenotype in zebrafish. EMBO Rep 3(7):688-694.

Gerety SS, Wang HU, Chen ZF, Anderson DJ. 1999. Symmetrical mutant phenotypes of the receptor EphB4 and its specific transmembrane ligand ephrin-B2 in cardiovascular development. Mol Cell 4(3):403-414.

Giri A, Mok KY, Jansen I, Sharma M, Tesson C, Mangone G, Lesage S, Bras JM, Shulman JM, Sheerin UM, International Parkinson's Disease C, Diez-Fairen M, Pastor P, Marti MJ, Ezquerra M, Tolosa E, Correia-Guedes L, Ferreira J, Amin N, van Duijn CM, van Rooij J, Uitterlinden AG, Kraaij R, Nalls M, Simon-Sanchez J. 2017. Lack of evidence for a role of genetic variation in TMEM230 in the risk for Parkinson's disease in the Caucasian population. Neurobiol Aging 50:167 e111-167 e113.

He YC, Huang P, Li QQ, Sun Q, Li DH, Wang T, Shen JY, Chen SD. 2016. TMEM230 stop codon mutation is rare in parkinson's disease and essential tremor in eastern China. Mov Disord.

Hellstrom M, Phng, L.K., Hofmann, J.J., Wallgard, E., Coultas, L., Lindblom, P., Alva, J., Nilsson, A.K., Karlsson, L., Gaiano, N., et al. 2007. Dll4 signalling through Notch1 regulates formation of tip cells during angiogenesis. Nature 445:776-780.

Hofmann K. 1993. TMbase - A database of membrane spanning proteins segments. Biol Chem Hoppe-Seyler 374(166).

Hogan BM, Herpers, R., Witte, M., Heloteraؤ , H., Alitalo, K., Duckers, H.J., and Schulte-Merker, S. 2009. Vegfc/Flt4 signalling is suppressed by Dll4 in developing zebrafish intersegmental arteries. Development 136:4001-4009.

Isogai S, Lawson ND, Torrealday S, Horiguchi M, Weinstein BM. 2003. Angiogenic network formation in the developing vertebrate trunk. Development 130(21):5281-5290.

Kim MJ, Deng HX, Wong YC, Siddique T, Krainc D. 2017. The Parkinson's disease-linked protein TMEM230 is required for Rab8a-mediated secretory vesicle trafficking and retromer trafficking. Hum Mol Genet.

Kimmel CB, Ballard WW, Kimmel SR, Ullmann B, Schilling TF. 1995. Stages of embryonic development of the zebrafish. Dev Dyn 203(3):253-310.

Lawson ND, Scheer N, Pham VN, Kim CH, Chitnis AB, Campos-Ortega JA, Weinstein BM. 2001. Notch signaling is required for arterial-venous differentiation during embryonic vascular development. Development 128(19):3675-3683.

Lawson ND, Weinstein, B. M. 2002. In vivo imaging of embryonic vascular development using transgenic zebrafish. Dev Biol 248:307-31817.

Leslie JD, Ariza-McNaughton L, Bermange AL, McAdow R, Johnson SL, Lewis J. 2007. Endothelial signalling by the Notch ligand Delta-like 4 restricts angiogenesis. Development 134(5):839-844.

Lobov IB, Renard, R.A., Papadopoulos, N., Gale, N.W., Thurston, G.,Yancopoulos, G.D., and Wiegand, S.J. 2007. Delta-like ligand 4 (Dll4) is induced by VEGF as a negative regulator of angiogenic sprouting. Proc

Natl Acad Sci USA 104:3219-3224.

For Peer Review

Morcos PA. 2007. Achieving targeted and quantifiable alteration of mRNA splicing with Morpholino oligos. Biochem Biophys Res Commun 358(2):521-527.

Nasevicius A, Ekker SC. 2000. Effective targeted gene 'knockdown' in zebrafish. Nat Genet 26(2):216-220.

Olszewska DA, Fearon C, Lynch T. 2016. Novel gene (TMEM230) linked to Parkinson's disease. J Clin Mov Disord 3:17.

Parsons MJ, Pisharath H, Yusuff S, Moore JC, Siekmann AF, Lawson N, Leach SD. 2009. Notch-responsive cells initiate the secondary transition in larval zebrafish pancreas. Mech Dev 126(10):898-912.

Phng LK, Gerhardt H. 2009. Angiogenesis: a team effort coordinated by notch. Dev Cell 16(2):196-208.

Quadri M, Breedveld GJ, Chang HC, Yeh TH, Guedes LC, Toni V, Fabrizio E, De Mari M, Thomas A, Tassorelli C, Rood JP, Saddi V, Chien HF, Kievit AJ, Boon AJ, Stocchi F, Lopiano L, Abbruzzese G, Cortelli P, Meco G, Cossu G, Barbosa ER, Ferreira JJ, International Parkinsonism Genetics N, Lu CS, Bonifati V. 2017. Mutations in TMEM230 are not a common cause of Parkinson's disease. Mov Disord.

Roman BL, Pham VN, Lawson ND, Kulik M, Childs S, Lekven AC, Garrity DM, Moon RT, Fishman MC, Lechleider RJ, Weinstein BM. 2002. Disruption of acvrl1 increases endothelial cell number in zebrafish cranial vessels. Development 129(12):3009-3019.

Schiavone M, Rampazzo E, Casari A, Battilana G, Persano L, Moro E, Liu S, Leach SD, Tiso N, Argenton F. 2014. Zebrafish reporter lines reveal in vivo signaling pathway activities involved in pancreatic cancer. Dis Model Mech 7(7):883-894.

Shutter JR, Scully S, Fan W, Richards WG, Kitajewski J, Deblandre GA, Kintner CR, Stark KL. 2000. Dll4, a novel Notch ligand expressed in arterial endothelium. Genes Dev 14(11):1313-1318.

Siekmann AF, Lawson ND. 2007. Notch signalling limits angiogenic cell behaviour in developing zebrafish arteries. Nature 445(7129):781-784.

Tammela T, Zarkada G, Wallgard E, Murtomaki A, Suchting S, Wirzenius M, Waltari M, Hellstrom M, Schomber T, Peltonen R, Freitas C, Duarte A, Isoniemi H, Laakkonen P, Christofori G, Yla-Herttuala S, Shibuya M, Pytowski B, Eichmann A, Betsholtz C, Alitalo K. 2008. Blocking VEGFR-3 suppresses angiogenic sprouting and vascular network formation. Nature 454(7204):656-660.

Thisse C, Thisse B, Schilling TF, Postlethwait JH. 1993. Structure of the zebrafish snail1 gene and its expression in wild-type, spadetail and no tail mutant embryos. Development 119(4):1203-1215.

Thompson MA, Ransom DG, Pratt SJ, MacLennan H, Kieran MW, Detrich HW, 3rd, Vail B, Huber TL, Paw B, Brownlie AJ, Oates AC, Fritz A, Gates MA, Amores A, Bahary N, Talbot WS, Her H, Beier DR, Postlethwait JH, Zon LI. 1998. The cloche and spadetail genes differentially affect hematopoiesis and vasculogenesis. Dev Biol 197(2):248-269.

Tusnady GE, Simon I. 2001. The HMMTOP transmembrane topology prediction server. Bioinformatics 17(9):849-850.

For Peer Review

Wang HU, Chen, Z. F. and Anderson, D. J. . 1998. Molecular distinction and angiogenic interaction between embryonic arteries and veins revealed by ephrin-B2 and its receptor Eph-B4. . Cell 93:741-753.

.

Westerfield M. 1993. The zebrafish book. Eugene OUoOP, editor.

Wu H, Zheng X, Cen Z, Xie F, Chen Y, Lu X, Luo W. 2016. Genetic analysis of the TMEM230 gene in Chinese patients with familial Parkinson disease. Parkinsonism Relat Disord.

Wu HH, Brennan C, Ashworth R. 2011. Ryanodine receptors, a family of intracellular calcium ion channels, are expressed throughout early vertebrate development. BMC Res Notes 4:541.

Yan W, Tang B, Zhou X, Lei L, Li K, Sun Q, Xu Q, Yan X, Guo J, Liu Z. 2017. TMEM230 mutation analysis in Parkinson's disease in a Chinese population. Neurobiol Aging 49:219 e211-219 e213.

Yaniv K, Isogai S, Castranova D, Dye L, Hitomi J, Weinstein BM. 2006. Live imaging of lymphatic development in the zebrafish. Nat Med 12(6):711-716.

For Peer Review

Figure legends

Figure 1. Genomic context of the *tmem230* family across selected species and gene structure analysis of zebrafish *tmem230a* and *tmem230b*. (a) The genomic context of zebrafish *tmem230a* with its orthologous and paralogous gene *tmem230b*. The gene placed in the center of the panel and aligned over the vertical line is the reference gene used as query (*tmem230a*). Blue square nodes (left part of the figure) represent ancestral species leading from the same root ancestral species to orthologs and/or paralogs of the gene used as query. Red square nodes represent duplication events of an ancestral version of the gene used as query. Open blue square nodes represent extant species. Upper thicker blue line represents the path leading from the ancestral root to the reference species used as query. Genes indicated by the same color are paralogs (without black boundary) or orthologs (black boundary). The figure was derived from the output of the Genomicus website (version 83.01). (**b**) Schematic representation of genes *tmem230a* and *tmem230b*.

Exons are indicated by blue boxes (for untranslated sequences) or orange boxes (for coding sequences) and introns are indicated by lines. Intron and exon lengths are not to scale. Lengths are shown in base pairs (bp). Exon-intron structure is derived from the Ensembl Genome Browser.

Figure 2. Spatio-temporal expression of zebrafish *tmem230a*. (**a**) *tmem230a* is expressed both maternally and zygotically during development. *tmem230a* and β-*actin* qualitative RT-PCR expression analysis on total RNA from oocytes, and various embryonic and larval stages (from 1-8 cells to 5 dpf) and adult organs and tissues. Negative control is no cDNA. The sizes of the PCR fragments are indicated. DNA Marker is a 1Kb ladder. (**b-j**) Whole Mount In Situ Hybridization (WISH) of *tmem230a* during embryo development. (**b-d, f** and **g**) Lateral views. (**b**) 15 somite stage embryo (after yolk removal), white arrowhead: forming axial vasculature. (**c**) 26 hpf embryo and (**c'**) higher magnification of the tail shows the expression in the CV, black arrowhead: CV. (**d**) Magnification of the head of a 26 hpf embryo, red arrowhead: the pharyngeal arch mesenchyme. (**e**) Dorsal and (**f**) lateral magnifications of the head, white asterisks: fin bud, and (**g**) lateral magnification of the tail of a 2 dpf embryo. Embryos are shown anterior to the left (**b-g**) Magnifications 40X and 63X. Transverse sections at the level of the trunk (**h**) and the tail (**i**) of a 26 hpf embryo, and tail (**j**) of a 2 dpf embryo. Histological analysis shows the signal in the DA: Dorsal Aorta, PCV: Posterior Cardinal Vein and CV: Caudal Vein. NC: Notochord. Magnification 280X.

For Peer Review

Figure 3. *tmem230a*-MO1 injection increases endothelial cell number within the ISVs. (**a,b**) Bright-field images of 29 hpf embryos injected with (**a**) std-MO and (**b**) *tmem230a*-MO1. Boxed areas indicate the ISVs considered for endothelial cell count. Magnification 40X. (**c-d**) Confocal fluorescent images of the tail of tg(*fli1*:nEGFP)^{y7}embryos injected with (**c**) std-MO and (**d**) *tmem230a*-MO1. Numbers indicate the cells within an ISV. Cell number is obtained by counting nuclei as the tg(*fli1*:nEGFP)^{y7}embryos display GFP in nuclei of *fli1* expressing cells. Magnification 20X. (**e**) Quantitative analysis of the cell number within the ISVs of 29 hpf tg(*fli1*:nEGFP)^{y7} embryos injected with std-MO and *tmem230a*-MO1. The number of analysed embryos is indicated by n. *** $p<0.001$ vs std-MO. (**f,g**) Cross sections of the trunk of 29 hpf embryos injected with (**f**) std-MO or (**g**) *tmem230a*-MO1. NC: NotoChord, DA: Dorsal Aorta, and PCV: Posterior Cardinal Vein. Magnification 350X. Horizontal line with cap is the mean ± s.e.m.

(**h-j**) Confocal fluorescent images of the tail of 29 hpf tg(*fli1*:nEGFP)^{y7}embryos injected with (**h**) 1 pmol/embryo of std-MO, (**i**) 1 pmol/embryo of *tmem230a*-MO2 or (**j**) 400 pg/embryo of *tmem230a* mRNA. Numbers indicate cells within an ISV. **(k,l)** Quantitative analysis of the cell number within the ISVs in 29 hpf tg(*fli1*:nEGFP)^{y7}embryos injected with (**k**) std-MO, *tmem230a*-MO1 or *tmem230a* mRNA, or with **(l)** std-MO, or *tmem230a*-MO2 on its own or in combination with *tmem230a* mRNA. The number of injected embryos analysed is n. *** $p<0.001$ vs std-MO (**k**) and *** $p<0.001$ vs MO2 (**l**). Horizontal line with cap is the mean ± s.e.m. Magnification 20X.

For Peer Review

30

Figure 4. *tmem230a* morphants display an increase of tip cell markers. (**a-j**) Expression analysis of *efnb2a*, e*phB4*, *flk1*, *flt4* and *dll4* performed on 29 hpf embryos injected with (**a,c,e,g** and **i**) std-MO or (**b**,**d**,**f**,**h** and **j**) MO1. Lateral views of the trunk region with anterior to the left. Red arrowhead: DA, cyan arrowhead: posterior CV, black arrowhead: DLAV, and white arrowhead: ISV. Magnification 63X.

Figure 5. *tmem230a* acts synergistically with the Dll4/Notch pathway in regulating ISV cell number. (**a-d**) Confocal fluorescent images of the tail of 29 hpf tg(*fli1*:nEGFP)^{y7}embryos injected with (**a**) 0.4 pmol/embryo of std-MO; (**b**) 0.4 pmol/embryo of *dll4*-MO; (**c**) 0.07 pmol/embryo (subcritical dose) of *tmem230a*-MO1 together with 0.09 pmol/embryo (subcritical dose) *dll4*-MO; and (**d**) 400 pg/embryo of *tmem230a* mRNA together with 0.4 pmol/embryo *dll4*-MO. In **a-d** numbers indicate the cells within a representative ISV. Magnification 20X. (**e-f**) Quantitative analysis of the cell number within the ISVs of 29 hpf tg(*fli1*:nEGFP)^{y7}embryos. (**e**) Embryos were injected with std-MO, or subcritical dose of *tmem230a*-MO1, or subcritical dose of *dll4*-MO, or subcritical dose of *tmem230a*-MO1 together with subcritical dose of *dll4*-MO. *** $p<0.001$ vs std-MO, vs *tmem230a*-MO1 and vs *dll4*-MO. (**f**) Embryos were injected with 0.4 pmol/embryo *dll4*-MO on its own and together with *tmem230a* mRNA. *** $p<0.001$ vs *dll4*-MO. (**g**) Embryos were injected with std-MO or *tmem230a* mRNA and then treated with DAPT. *** $p<0.001$ vs std-MO + DAPT. Control embryos (std-MO) and *tmem230a* mRNA injected embryos were treated with the same concentration of DMSO as DAPT immersed embryos. The number of injected embryos analysed is n. Horizontal line with cap is the mean ± s.e.m.

30

For Peer Review

Figure 6. *tmem230a*-MO1 injection inhibits Notch signalling activation in vessels. (**a-d**) Analysis of mCherry expression in vessels of 48 hpf embryos derived from the transgenic line tg(T2KTp1bglob:hmgb1-mCherry)^{jh11} crossed with the transgenic line tg(*fli1*:EGFP)^{y1}; injected with std-MO (**a**,**b**) or *tmem230a*-MO1 (**c**,**d**). ISV: InterSomitic Vessel, and DA: Dorsal Aorta. Magnification 40X.

For Peer Review

Supplementary Figure 1. Tmem230 protein analysis.

(**a**) Amino acid identity and similarity (in parentheses) between zebrafish (*Danio rerio*) Tmem230a and Tmem230b and human and mouse ortholog proteins: *Homo sapiens* (gi:42476068) and *Mus musculus* (gi:213972600). (**b**) Topology prediction analysis of conserved domains revealed that Tmem230a and Tmem230b proteins contain 2 transmembrane domains.

Supplementary Figure 2. Spatio-temporal expression pattern of zebrafish *tmem230b*.

(**a**) *tmem230b* and β–*actin* qualitative RT-PCR expression analysis on total RNA from oocytes, and embryonic and larval stages (from 1-8 cells to 5 dpf) and different adult

organs and tissues. DNA Markers are 100 bp ladder and 1Kb ladder. Negative control is no cDNA. The sizes of the PCR fragments are indicated. *tmem230b* is expressed both maternally and zygotically in embryo development. (**b-f**) WISH analysis of *tmem230b* at various developmental stages. (**b**) Lateral view of a 15 and of a (**c**) 20 somite stage embryo, white arrowhead: somites. (**d**) Lateral view of a 26 hpf embryo and (**d'**) higher magnification of the tail shows the expression of *tmem230b* in the CV region and somites, red arrowhead: somites and black arrowhead: CV region. Head at (**e**) 26 hpf and at (**f**) 2 dpf. Embryos are shown anterior to the left. Magnifications 40X and 63X.

Supplementary Figure 3. MO1 and MO2 are designed to specifically target the *tmem230a* transcript.

(**a**) Sequence alignments obtained with CLUSTAL W, between *tmem230a* and *tmem230b, tmem230a* and *tmem230b* with the sequences of *tmem230a*-MO1 and *tmem230a* and *tmem230b* with *tmem230a*-MO2 demonstrate the specificity of the MOs with the *tmem230a* sequence. Green box shows translation start sites. (**b**) Schematic representation of the position of *tmem230a*-MO1 and *tmem230a*-MO2 binding to *tmem230a* mRNA. Exon and intron lengths are indicated. The effectiveness of the splice-blocking morpholino, *tmem230a*-MO2 designed to target exon 2 was shown by the generation of an amplification product that excludes exon 2 using forward (For.) and reverse (Rev.) primers designed in the first and last exons. Injection of splice-blocking *tmem230a*-MO2 results in the generation of a smaller product (in red box) corresponding to the *tmem230a* transcript lacking exon 2. The sizes of the PCR fragments are indicated. DNA Marker is a 1Kb ladder.

For Peer Review

Supplementary Figure 4. Dose-response of *tmem230a*-MO1 on embryo survival and morphological defects and dose-response of *tmem230a*-MO2 on ISV cell number.

(**a**) Survival and morphological defects (bent tail and small head) histograms of tg(*fli1*:nEGFP)^{y7}embryos at 29 hpf injected with different doses of *tmem230a*-MO1. (**b**) Quantitative analysis of cell number in the ISVs for tg(*fli1*:nEGFP)^{y7}embryos injected with std-MO and different doses of *tmem230a*-MO2 at 29 hpf. The number of injected embryos is n. ** $p<0.01$ vs std-MO.

Supplementary Figure 5.

***tmem230a*-MO1 injection causes no gross effects on vasculogenesis and angiogenesis at 2 dpf.** *In vivo* analysis of tg(*fli1*:EGFP)^{y1} embryos injected with (**a-d**) std-MO or (**e-h**) *tmem230a*-MO1. (**a**,**b**,**e** and **f**) Bright field and (**c**,**d**,**g** and **h**) fluorescence images. Magnification of the caudal region (**b**,**d**,**f**, and **h**). Lateral views are shown anterior to the left. DLAVs: Dorsal Longitudinal Anastomotic Vessels, ISVs: Intersomitic Vessels, DA: Dorsal Aorta, and CV: Caudal Vein. Magnifications 25X and 63X.

For Peer Review

Figure 1 (Zucchi et al 2016)

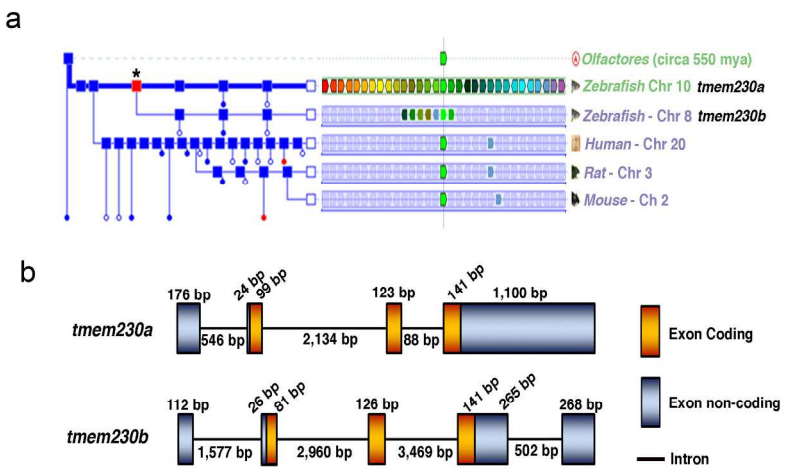

Figure 1. Genomic context of the tmem230 family across selected species and gene structure analysis of zebrafish tmem230a and tmem230b.
Figure 1. Genomic context of t
254x317mm (300 x 300 DPI)

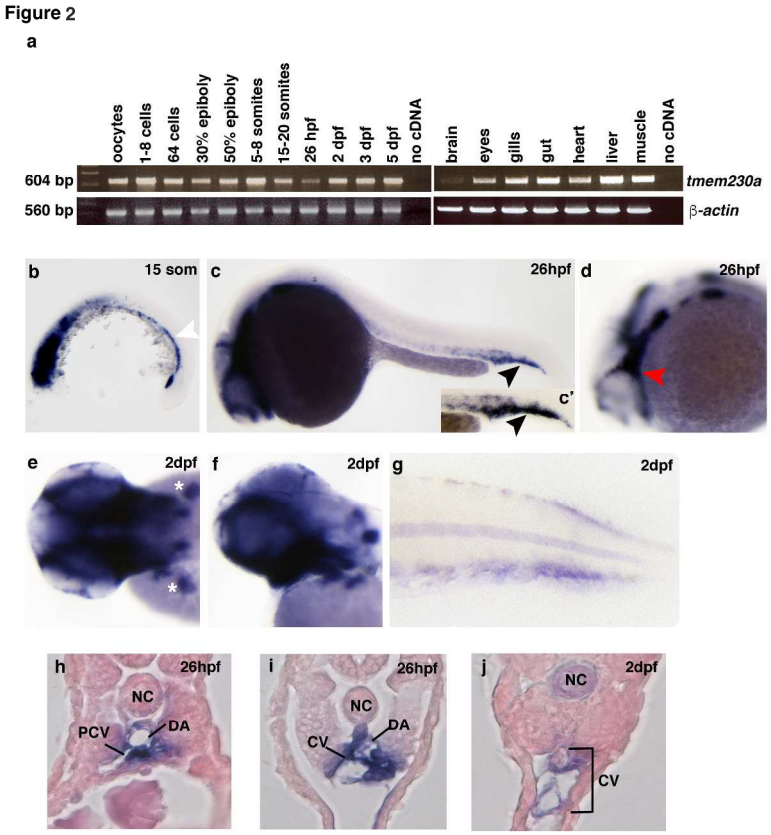

Figure 1. Genomic context of the tmem230 family across selected species and gene structure analysis of zebrafish tmem230a and tmem230b.
Figure 1. Genomic context of t
275x361mm (300 x 300 DPI)

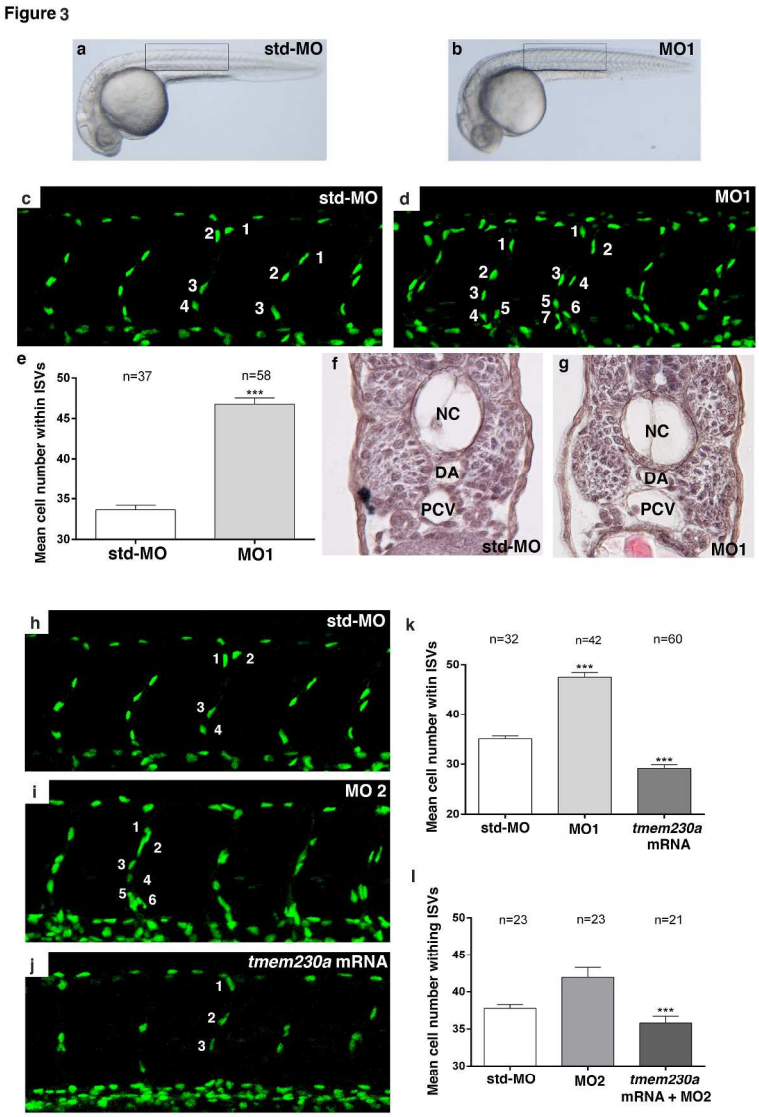

Figure 3. tmem230a-MO1 injection increases endothelial cell number within the ISVs.
Figure 3. tmem230a-MO1 injecti
297x420mm (300 x 300 DPI)

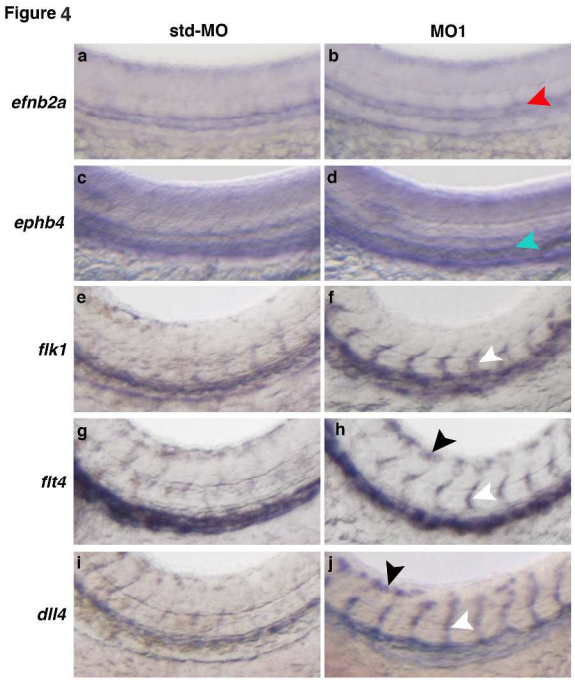

Figure 4. tmem230a morphants display an increase of tip cell markers.
Figure 4. tmem230a morphants d
297x420mm (300 x 300 DPI)

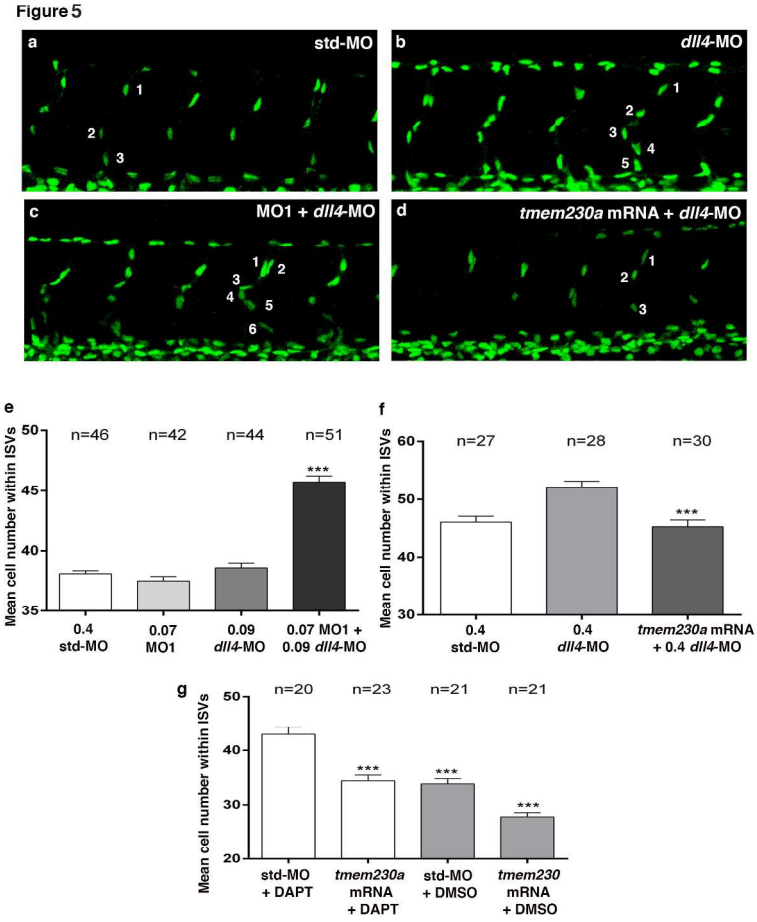

Figure 5. tmem230a acts synergistically with the Dll4/Notch pathway in regulating ISV cell number.
Figure 5. tmem230a acts synerg
209x297mm (300 x 300 DPI)

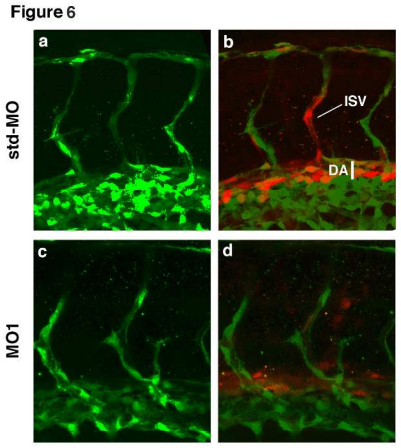

Figure 6. tmem230a-MO1 injection inhibits Notch signalling activation in vessels.
Figure 6. tmem230a-MO1 injecti
209x297mm (300 x 300 DPI)